Inorg. Chem. **2009**, *48*, 1293−1300

Synthesis and Characterization of Lithium Hemiporphyrazines

Saovalak Sripothongnak,[†] Anna M. Pischera,[†] Matthew P. Espe,[†] William S. Durfee,[‡] and Christopher J. Ziegler*[,†]

Department of Chemistry, University of Akron, Akron, Ohio 44325-3601, and Department of Chemistry, Buffalo State College, Buffalo, New York 14222

Received May 5, 2008

The hemiporphyrazines comprise a broad class of phthalocyanine analogues where one or two of the diiminoisoindolene units are replaced with alternative rings, including pyridines, benzenes, and azoles. As a means to explore the fundamental metal chemistry of these macrocycles, we have prepared the first lithium complexes of three hemiporphyrazine variants: the common bis-pyridine ring, the bis-benzene macrocycle (also known as dicarbahemiporphyrazine), and the monobenzene variant (also known as benziphthalocyanine). The metal cation can be inserted via reaction of the free bases by using lithium bis(trimethylsilyl)amide, and the resulting products all form 1:1 complexes with protonation at the meso nitrogens providing charge balance. For the two carbahemiporphyrazines studied, the internal C−H bond remains intact upon metalation. Similar structures have been observed in the transition metal complexes of the carbaporphyrins. In addition, all three complexes are characterized by ^{7}Li solid state NMR and by cyclic voltammetry.

Over the past century, metalloporphyrins and metallophthalocyanines have played central roles in coordination chemistry.[1] These macrocycles have been used as models for biologically active sites,[2] as catalysts for organic transformations,[3] and as materials for both simple and advanced applications.[4] Accordingly, the metalation chemistry for both porphyrins and phthalocyanines has been extensively developed, and a wide variety of metal insertion reaction types have appeared in literature.[5] One of the more recently studied methods for incorporating a metal into a porphyrin has been the use of lithium based intermediates.[6] Lithium porphyrins react with a variety of metal salts, resulting in a metathesis of the lithium cation to produce the desired metal porphyrin adduct. For example, this method is very useful for the generation of the early transition metal ion porphyrins since these compounds often cannot be made by direct reaction of the free base in the presence of a source of the metal.[7] In the phthalocyanines, lithiated macrocycles have been investigated as advanced materials for photosensitive and oximetric compounds.[8]

In contrast to the metalation chemistry of normal porphyrins and phthalocyanines, the insertion of metals into porphyrin analogues and isomers continues to be an open area of investigation. The isomers and analogues of porphyrin and phthalocyanine present challenges for metalation that are not present in normal porphines or azaporphyrins. Many of the skeletal modified porphyrins are not as stable as normal porphine and are not robust enough to survive harsh

* To whom correspondence should be addressed. E-mail: ziegler@uakron.edu.

[†] University of Akron.

[‡] Buffalo State College.

(1) (a) *The Porphyrin Handbook*; Kadish, K. M., Smith, K. M., Guilard R., Eds.; Academic Press: New York, 2000; Vol. *1*−*10*. (b) *Phthalocyanines: Properties and Applications*; Leznoff, C. C., Lever, A. B. P., Eds.; VCH: Weinheim, Germany, 1989.

(2) (a) Momenteau, M.; Rougée, M.; Loock, B. *Eur. J. Biochem.* **1976**, *71*, 63. (b) Fiammengo, R.; Wojciechowski, K.; Crego-Calama, M.; Timmerman, P.; Figoli, A.; Wessling, M.; Reinhoudt, D. N. *Org. Lett.* **2003**, *5*, 3367.

(3) (a) Bhyrappa, P.; Krishnan, V. *Inorg. Chem.* **1991**, *30*, 239. (b) Liu, Y.; Zhang, H.-J.; Lu, Y.; Cai, Y.-Q.; Liu, X.-L. *Green Chem.* **2007**, *9*, 1114. (c) Chen, W.; Lu, W.; Yao, Y.; Xu, M. *Environ. Sci. Technol.* **2007**, *41*, 6240.

(4) (a) Wang, L.; Liu, G. *Appl. Phys. Lett.* **2007**, *91*, 153508. (b) Jang, J. H.; Jeon, K.-S.; Oh, S.; Kim, H.-J.; Asahi, T.; Masuhara, H.; Yoon, M. *Chem. Mater.* **2007**, *19*, 1984. (c) Claessens, C.; Hahn, U.; Torres, T. *Chem. Rec.* **2008**, *8*, 75–97. (d) Nyokong, T. *Coord. Chem. Rev.* **2007**, *251*, 1707–1722. Kim, D.; Osuka, A. *Acc. Chem. Res.* **2004**, *37*, 735–745.

(5) Buchler, J. W. In *The Porphyrins*; Dolphin, D., Ed.; Academic Press: New York, 1979; Vol. *1*, p 389.

(6) (a) Brand, H.; Capriotti, J. A.; Arnold, J. *Inorg. Chem.* **1994**, *33*, 4334. (b) Arnold, J.; Dawson, D. Y.; Hoffman, C. G. *J. Am. Chem. Soc.* **1993**, *115*, 2707.

(7) Berreau, L. M.; Hays, J. A.; Young, V. G.; Woo, L. K. *Inorg. Chem.* **1994**, *33*, 105.

(8) (a) Gilat, S. L.; Ebbesen, T. W. *J. Phys. Chem.* **1993**, *97*, 3551. (b) Bensebaa, F.; Andre, J. J. *J. Phys. Chem.* **1992**, *96*, 5739. (c) Sato, H.; Dalton, L. A.; Ha, D.; Quine, R. W.; Eaton, S. S.; Eaton, G. R. *J. Phys. Chem. B* **2007**, *111*, 7972.

10.1021/ic800817x CCC: $40.75
Published on Web 01/15/2009

Scheme 1

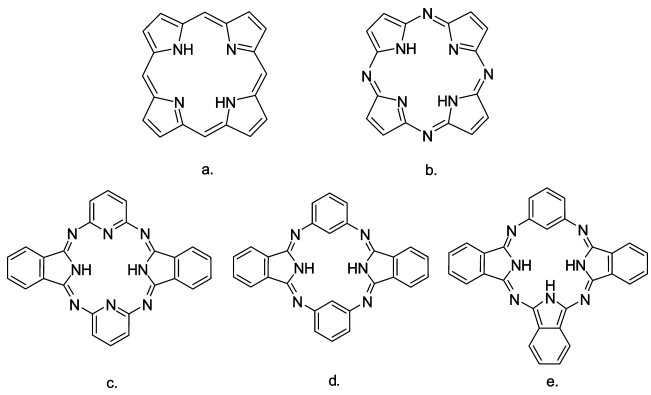

metalation conditions.[9] Alternatively, core modified porphyrins can be difficult to metalate due to the presence of weakly binding heteroatoms, such as sulfur in the thiaporphyrins.[10] The carbaporphyrins can also be challenging to metalate because of the presence of carbon at the metal binding site, as seen in N-confused porphyrin, azuliporphyrin, or benziporphyrin.[11] However, in spite of these difficulties, significant metalation literature has been developed for several porphyrin analogues and isomers, including corrole[12] and N-confused porphyrin.[13]

We have recently begun to investigate the chemistry of the hemiporphyrazines, a family of phthalocyanine analogues where one or two isoindolene units are replaced with alternative rings (Scheme 1).[14] In normal porphyrin (a) and azaporphyrin (b), the ring is composed of four conjugated pyrrole units, linked by bridging meso carbons and nitrogens respectively. Examples of the hemiporphyrazines include normal hemiporphyrazine (c),[15] where pyridines have been introduced into the macrocycle, dicarbahemiporphyrazine (d),[16] where benzene rings replace the pyridyl rings, and benziphthalocyanine (e),[17] where a single benzene ring is substituted for an isoindolene unit. The metalation chemistry of normal hemiporphyrazine has been developed,[14] but not to the extent of either porphyrin or normal phthalocyanine. In contrast, the metalation chemistry of dicarbahemiporphyrazine and benziphthalocyanine was until recently largely unexplored; we have published some of the first crystallographic structural characterization in this area.[18] All three macrocycles exhibit reduced stability versus normal porphyrin and azaporphyrin. The macrocycles are not aromatic and can be hydrolytically cleaved in the presence of acid. In addition, dicarbahemiporphyrazine and benziphthalocyanine are both carbaporphyrins, and the presence of the internal C−H groups inhibits metalation. Lastly, all three free base macrocycles have very poor solubility, which frequently limits the solvents that can be used to work with these rings.

In this report, we present the lithium chemistry of hemiporphyrazine (hp), dicarbahemiporphyrazine (dchp), and benziphthalocyanine (bzpc). The lithium adducts of all three macrocycles can be readily generated, and we have structurally characterized the three by single crystal X-ray methods. In all cases, only a single lithium inserts into the ring, and in the cases of the carbaporphyrinoids, the internal C−H bonds remain intact. Also, the formation of the lithium adducts significantly increases the solubilities of these rings, and we believe that these reagents will greatly assist investigations into the metalation chemistry of these macrocycles.

Results and Discussion

The lithium chemistry of both normal porphyrin and azaporphyrins, including phthalocyanines, has been previously explored.[6,19] These two macrocycle types can bind the lithium cation in distinctly different modes. The lithium complexes of porphyrins typically have an M_2P stoichiometry, and different binding modes of the monovalent cation can be observed. This chemistry is dependent on both the identity of the solvent and the nature of the peripheral substitution on the porphyrin ring. For the complex $Li_2(THF)_4(OEP)$, a single lithium binds to the core of the ring while a second equivalent of cation is coordinated by four solvent tetrahydrofuran (THF) molecules in a tetrahedral geometry. In addition, in nonpolar solvents, a nonionic structure is adopted, where the lithium ions bind to the ring in symmetric out-of-plane structures. In contrast, the lithium complexes of the azaporphyrins show symmetric in-plane binding of the cation. In all cases, the macrocycle remains dianionic, and a second equivalent of cation (tetraalkylammonium, bis(triphenylphosphin)iminium, or $Li(L)_4$) is required for charge balance. In addition, there has been structural investigation of the Li(*Pc*) radical anion, and in these cases the lithium also resides squarely in the core of the macrocycle. Four decades ago, Kenney and Sutton reported on the reaction of LiH with the bis(pyridyl)hemiporphyrazine and isolated two products by crystallization and sublimation; the products were characterized only by elemental analysis and IR spectroscopy.[20]

(9) *Expanded, Contracted and Isomeric porphyrins*; Sessler, J. L., Weghorn, S. J., Eds.; Elsevier Science: New York, 1997.
(10) Chmielewski, M. J.; Pawlicki, M.; Sprutta, N.; Szterenberg, L.; Latos-Grażyński, L. *Inorg. Chem.* **2006**, *45*, 8664.
(11) (a) Harvey, J. D.; Ziegler, C. J. *J. Inorg. Biochem.* **2006**, *100*, 869. (b) Harvey, J. D.; Ziegler, C. J. *Coord. Chem. Rev.* **2003**, *247*, 1. (c) Lash, T. D.; Colby, D. A.; Graham, S. R.; Ferrence, G. M.; Szczepura, L. F. *Inorg. Chem.* **2003**, *42*, 7326. (d) Myśliborski, R.; Latos-Grażyński, L. *Eur. J. Org. Chem.* **2005**, 5039.
(12) Gross, Z. *J. Bio. Inorg. Chem.* **2001**, *6*, 733.
(13) Chmielewski, P. J.; Latos-Grażyński, L. *Coord. Chem. Rev.* **2005**, *249*, 2510.
(14) Fernández-Lázaro, F.; Torres, T.; Hauschel, B.; Hanack, M. *Chem. Rev.* **1998**, *98*, 563.
(15) Elvidge, J. A.; Linstead, R. P. *J. Chem. Soc.* **1952**, 5008.
(16) Clark, P. F.; Elvidge, J. A.; Linstead, R. P. *J. Chem. Soc.* **1954**, 2490.
(17) Elvidge, J. A.; Golden, J. H. *J. Chem. Soc.* **1957**, 700.
(18) (a) Çetin, A.; Durfee, W. S.; Ziegler, C. J. *Inorg. Chem.* **2007**, *46*, 6239. (b) Wu, R.; Çetin, A.; Durfee, W. S.; Ziegler, C. J. *Angew. Chem., Int. Ed.* **2006**, *45*, 5670. (c) Çetin, A.; Sripothongnak, S.; Kawa, M.; Durfee, W. S.; Ziegler, C. J. *Chem. Commun.* **2007**, *41*, 4289.
(19) (a) Sugimoto, H.; Mori, M.; Masuda, H.; Taga, T. *Chem. Commun.* **1986**, 962. (b) Latte, B.; Kienast, A.; Bruhn, C.; Loidl, A.; Homborg, H. *J. Porphyrins Phthalocyanines* **1997**, *1*, 267. (c) Homborg, H.; Teske, C. L. *Z. Anorg. Allg. Chem.* **1985**, *527*, 45. (d) Hückstädt, H.; Jaouen, C.; Göldner, M.; Cornelissen, U.; Tutass, A.; Homborg, H. *Z. Anorg. Allg. Chem.* **2000**, *626*, 671. (e) Latte, B.; Assmann, B.; Homborg, H. *Z. Anorg. Allg. Chem.* **1997**, *623*, 1281. (f) Assmann, B.; Franken, A.; Homborg, H. *Z. Anorg. Allg. Chem.* **1995**, *621*, 1715. (g) Gebauer, A.; Schmidt, J. A. R.; Arnold, J. *Inorg. Chem.* **2000**, *39*, 3424. (h) Popov, K.; Lajunen, L. H. J.; Popov, A.; Rönkkömäki, H.; Hannu-Kuure, M.; Vendilo, A. *Inorg. Chem. Commun.* **2002**, 223. (i) Arnold, J. *Chem. Commun.* **1990**, 976.

Scheme 2

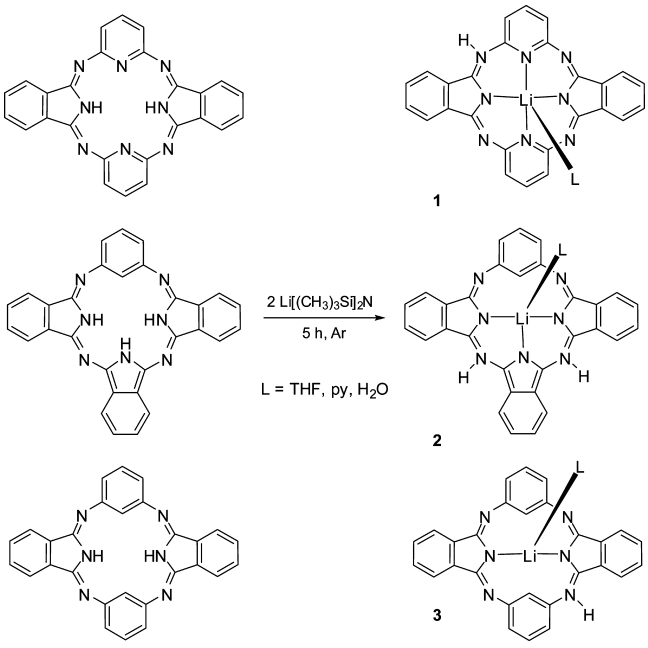

The lithium adducts of the three hps shown in Scheme 1 can be readily produced via the reaction of lithium bis(trimethylsilyl)amide and the free base macrocycle in THF (Scheme 2). In all cases, compounds **1**−**3** are monolithium adducts, and the use of excess amounts of lithium bis(trimethylsilyl)amide does not result in the formation of other stoichiometries, regardless of the number of protons present in the core of the macrocycle. In all cases, the lithium is coordinated in the axial position by a solvent ligand, and the identity of this axial species is determined by the conditions of recrystallization. Product isolation from anhydrous pyridine and anhydrous THF results in the two solvents occupying the axial position, while exposure to small amounts of water (such as from nonanhydrous THF) results in a water molecule binding. Charge balance is provided by the presence of one or more protons at meso nitrogen positions. As a result, we can consider these rings to have a positive charge at the exterior protonated meso nitrogen atoms, which balances the negative charge at the internal deprotonated isoindolene nitrogen atoms. Similar protonations have been observed in the silver complex of dchp and in the cobalt complexes of bzpc.[18] Such meso nitrogen protonation is not seen in the lithium complexes of the azaporphyrins or the phthalocyanines, whereas the Schiff base sites in the hp can be readily protonated.

In contrast to the free base bis(pyridyl)hemiporphryazine, the lithium adduct is much more soluble in organic solvents. The free base has limited solubility in THF, but as the reaction proceeds, the unmetalated ring dissolves, affording a solution of the lithium adduct. Crystals of the pure product can be readily isolated upon diffusion with an alkane, and analysis of the product is consistent with the incorporation of a lithium in the core of the ring. The ^{7}Li NMR of the product shows a broad peak with a chemical shift of 1.96 ppm in pyridine (versus LiCl in D_2O; the bis(trimethylsilyl)amide lithium reagent shows a shift at 0.52 ppm in THF and 2.28 ppm in pyridine solvents). This chemical shift is in contrast to that observed in lithium porphyrins. The lithium adducts of porphyrins exhibit chemical shifts significantly upfield, between ∼1 ppm[19h] (for the $Li(THF)_4^+$ cations required for charge balance) and −16.5 ppm, versus LiCl in MeOH.[6b] In phthalocyanines, much of the synthesis has focused on radical complexes, rather than diamagnetic adducts.[19] Two factors contribute to the differences in chemical shift in lithium porphyrins: the coordination geometries of the metal and the aromatic ring current. In the five-coordinate lithium adduct of thiaporphyrin, the chemical shift is −10.15 ppm.[19g] The nonaromatic hp's clearly do not move the chemical shift downfield because of a diatropic ring current effect, with the exception of a small possible contribution from the pyridines.

Figure 1. Structure of hemiporphyrizinatopyridine lithium (**1**) with 35% thermal ellipsoids. Hydrogen atoms have been omitted for clarity.

Crystals of the lithium adduct of bis(pyridyl)hemiporphyrazine (**1**) were isolated via a pyridine/hexane layered diffusion process. The structure of this complex shows the lithium atom sitting within the core of the macrocycle, as can be seen in Figure 1. The four nitrogens of the ring are all bound to the cation, with bond distances of 1.978(3) and 1.997(3) Å for the diiminoisoindolenes and 2.193(3) and 2.352(3) Å for the pyridines. These bonds reflect a lack of symmetry in the macrocycle that arises due to the protonation at one of the four external Schiff base sites (vide infra). The molecule is not disordered, and the asymmetry is clearly visible in the structure elucidation. The lithium is five-coordinate, and the axial position is occupied by a single pyridine, with a Li−N bond distance of 2.144(3) Å.

The macrocycle deviates from planarity, with the two diiminoisoindolene nitrogen atoms pointing away from the lithium and the two pyridine nitrogen atoms tilted toward the axial pyridine. The diiminoisoindoline and pyridine rings are tilted away from their lithium−nitrogen bond ordinates; this results in a trigonal pyramidal geometry about each nitrogen atom at the core. This saddle shape adopted by the hp ligand resembles that seen in dchp free bases, where the benzene and diiminoisoindolene units alternatively deviate from the plane of the macrocycle. The four internal nitrogen

(20) Sutton, L. E.; Kenney, M. E. *Inorg. Chem.* **1967**, *6*, 1869–1872.

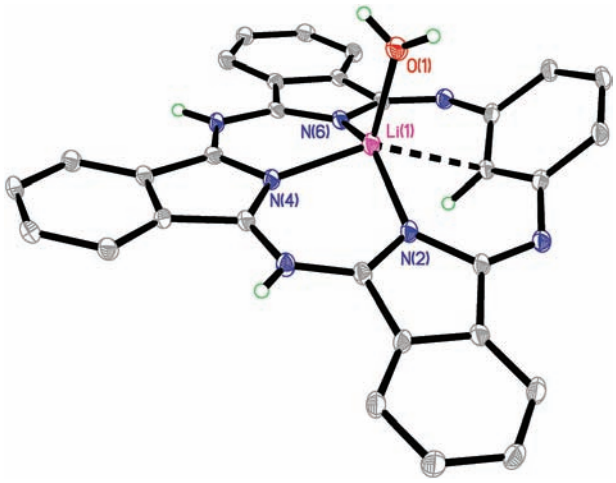

Figure 2. Structure of aquabenziphthalicyanato lithium (**2**) with 35% thermal ellipsoids. Hydrogen atoms have been omitted for clarity, except on the axial water, at the meso nitrogens and at the internal carbon site.

atoms reside within the same plane, but the two diiminoisoindolene rings are tilted down from the axial pyridine by ~17° and ~15°. The two pyridine rings in the hp backbone tilt up toward the axial pyridine by larger angles with one at ~40° to the plane of the four internal nitrogens and the second at ~29°. The larger tilt is observed with the pyridine immediately adjacent to the protonated Schiff base; the presence of the external proton imparts increased flexibility to this part of the ring. The lithium rises out of the plane defined by the four core nitrogen atoms toward the axial pyridine by ~0.49 Å.

As mentioned above, charge balance is provided by protonation of one of the external meso nitrogen positions; the hydrogen atom was located on the difference map during the structural elucidation. Further evidence for this proton can be found in the C−N bond distances to this meso position; they are appreciably longer than those observed for the proton-free meso positions. In addition, this proton is readily observed in the ^{1}H NMR at 10.74 ppm. In solution, all of the positions are equivalent, resulting in dynamic behavior and the broadening of this peak in the NMR spectrum.

Lithium also readily inserts into the bzpc macrocycle. As in the hp reaction, metalation results in increasing solubility, and the starting free base dissolves as the reaction proceeds. Pure metalated product can be produced upon diffusion of the THF solution with an alkane, and single crystals of this complex were isolated from nonanhydrous THF layered with hexanes. The structure of the bzpc adduct (**2**) is shown in Figure 2. The macrocycle remained metalated even in the presence of THF that was not dried prior to use, indicating that the complex is reasonably stable to water. However, it is important to note that we were unable to observe the complex by high resolution electrospray ionization mass spectrometry (ESI MS); only the demetalated product was detected. The lithium cation lies within the plane of the macrocycle and is coordinated by three nitrogens from the ring and by an axial water molecule adventitiously acquired from the THF. The Li−N bond distances average 2.051(4) Å for the diiminoisoindolenes adjacent to the benzene ring, and the distance is 1.959(4) Å for the bond opposite the benzene. The axial Li−O bond is 1.942(5) Å, which corresponds to an average Li−OH_2 bond length.

In the bzpc complex, the internal C−H bond is not deprotonated and forms an agostic-like bond to the metal center. Such bonding was first observed in benziporphryins with Ni(II) in 2004.[21] The Li−C bond is long (2.528(5) Å) and thus cannot be characterized as a strong organometallic interaction. However, the C−H bond does force the lithium cation out of the plane of the ring (as defined by the plane of the three internal nitrogens) by 0.63 Å and reduces the length of the opposite Li−N bond versus that of the adjacent Li−N bonds by ~0.09 Å. Similar trends have been observed in the metal complexes of the N-confused porphyrins, where the internal C−H bond frequently remains intact upon metalation.[11] The benzene ring of the bzpc is tilted away from the metal, at an angle of 41.9° from the plane of the three core nitrogens. The axial water−lithium bond also lies at an angle of 81.7° from this same plane, and the bond is tilted toward the benzene ring. This axial ligand tilt is directly analogous to that seen in the metal complexes of N-confused porphyrins that exhibit agostic-type interactions.

In contrast to the Li(hp)(py) complex described above, the Li(bzpc)(H_2O) macrocycle is surprisingly planar, with a small deviation induced by the out-of-plane location of the cation. As in the Li(hp)(py) compound, charge balance is provided by protonation of two meso nitrogen positions, and both hydrogens were located on the difference map. In addition, the location of these hydrogens was confirmed by inspection of the imine bond lengths, which lengthen upon protonation. In the ^{1}H NMR spectrum, the external protons are observed at 8.39 and 8.68 ppm, indicating that, in solution, protonation of the external meso nitrogens is dynamic and that the signals result from the two chemically inequivalent nitrogen positions. The internal C−H proton can be observed at 7.20 ppm, slightly downfield from that of the previously observed Ag(I) adduct of dchp.[18] We did not observe a ^{1}H−^{7}Li coupling constant in this species, presumably due to the quadrupolar moment of ^{7}Li. The ^{7}Li NMR of the product in THF shows a broad peak at 3.11 ppm, which demonstrates the nonaromatic character of the ring.

A yellow crystalline product is produced upon reaction of dchp with lithium bis(trimethylsilyl)amide. When crystallized from pyridine/hexanes, the crystals grow in two morphologies: large, highly twinned needles and small blocks that were suitable for single crystal X-ray structure elucidation. The structure of the lithium adduct from pyridine solution (**3**) is shown in Figure 3. The structure of this complex is similar to that previously seen for the transion metal ions Ag(I), Mn(II), Fe(II), and Co(II) and to that seen in the free base structure.[18,22] The lithium ion is coordinated by the two nitrogens from diiminoisoindolenes from the ring, with Li−N bond distances of 2.067(3) and 2.131(3) Å. The

(21) Stepien, M.; Latos-Grazynski, L.; Szterenberg, L.; Panek, J.; Latajka, Z. *J. Am. Chem. Soc.* **2004**, *126*, 4566.
(22) (a) Peng, S.-M. *Bull. Inst. Chem.* **1986**, *33*, 35. (b) Shishkin, O. V.; Kovalevsky, A. Y.; Shcherako, M. V.; Islyaikin, M. K.; Kudrik, E. V.; Baranski, A. *Kristallografiya* **2001**, *46*, 461.

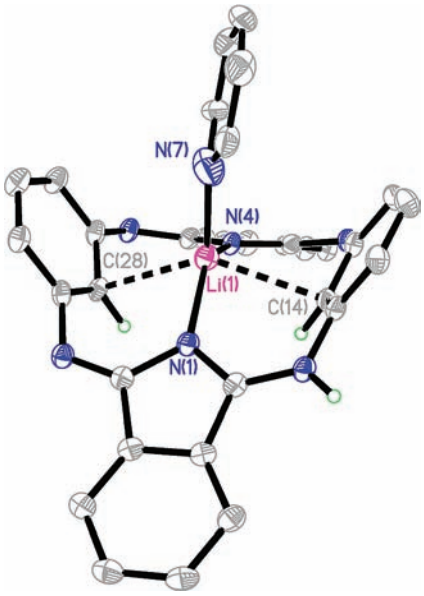

Figure 3. Structure of dicarbahemiporphyrazinato lithium (**3**) with 35% thermal ellipsoids. Hydrogen atoms have been omitted for clarity, except on the internal carbon positions and on the external meso nitrogen.

internal C−H bonds remain intact and remain in close proximity to the lithium center. These types of bonds have been described as agostic-type interactions in transition metal carbaporphyrin complexes.[11,18] As in the transition metal complexes of dchp, the Li−C bonds are long but within the van der Waal radii of the two elements (2.489(3) and 2.468(3) Å). As a result of the presence of the two internal C−H bonds, the macrocycle adopts a highly nonplanar saddle conformation. These two internal protons can be located on the difference map from the X-ray data. The axial position is coordinated by a single pyridine; in this crystal form, this axial solvent is disordered, and we modeled the axial pyridine by using two nearly coplanar orientations with slightly different tilts toward the bound diiminoisoindolene units. The axial Li−N bond distances for these two primary orientations are 1.950(15) and 2.062(10) Å.

The above-described coordination mode requires deprotonation of both nitrogens at the core, and to obtain a neutral complex, a meso nitrogen should be protonated at the ring periphery. We have observed this peak in the difference map in the elucidated structure, but in addition, this proton is readily observable in the ^{1}H NMR spectrum, appearing at 9.16 ppm. The internal protons in **3** are also slightly downfield from the corresponding Ag(I) complex, appearing at 7.22 ppm. Once again, we were not able to observe a ^{1}H−^{7}Li coupling constant. The mass spectrum exhibits peaks corresponding to an unsolvated lithium dchp, as well as the complex with a single aqua ligand. The elemental analysis of product recrystallized from nonanhydrous THF is consistent with the presence of both a THF and a water in the formula. The ^{1}H NMR for this same material shows peaks for both water and THF present in the structure, which is consistent with coordination of one or both solvents. We examined the ^{7}Li NMR spectrum of the product and observed broad peaks at 2.75 ppm in anhydrous THF and 1.54 ppm in anhydrous pyridine, which is consistent with the other hp

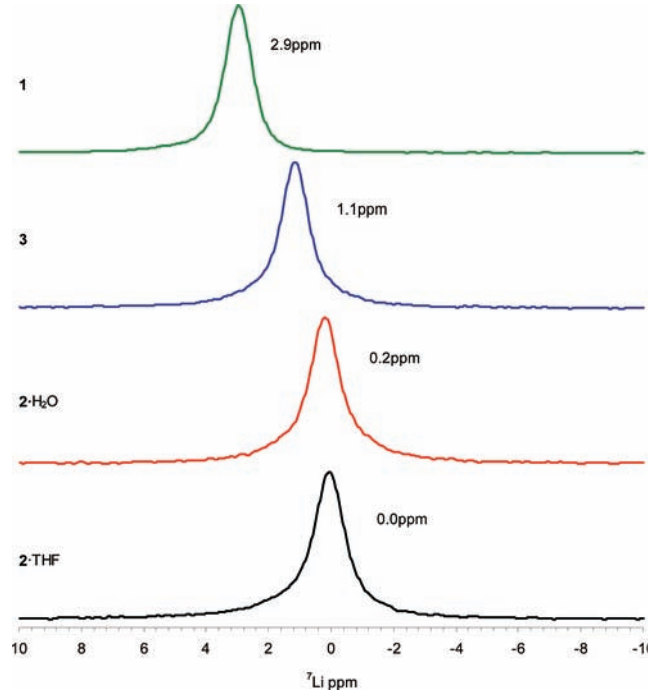

Figure 4. 155 MHz ^{7}Li solid-state MAS NMR spectra from compounds **1**−**3**. Only the central transition from each spectrum is shown.

lithium complexes presented in this report and surprisingly close to that of the bzpc adduct, which also exhibits an agostic-type interaction at the metal binding core.

The lithium sites in these compounds were also characterized by using ^{7}Li solid-state NMR (SSNMR), since the mechanisms that make collecting solution NMR data difficult, such as dynamic processes, ion pair formation, dimerization, and so forth, are eliminated.[23] While we are able to observe single ^{7}Li resonances for **1**−**3** in solution, we do not know the structure of these species in solution. In contrast, we can directly correlate the chemical shift to structure for SSNMR, since we have single crystal X-ray data for all three compounds. The ^{7}Li nucleus is quadrupolar with a nuclear spin of 3/2. The central transition, $+1/2 \rightarrow -1/2$, of the NMR spectrum occurs at the isotropic chemical shifts, and a peak will be generated for each unique species present. Second order quadrupole coupling interactions can cause a shift in the isotropic value,[24] but in this case, a shift of the isotropic peak of only 0.05 ppm is expected at the field strength used in these studies, so this effect can be ignored.[23] We examined four compounds: compounds **1** and **3** isolated from anhydrous pyridine and two samples of **2** from wet THF (with an axial water) and dry THF (with an axial THF). Each of the four compounds studied produces only one resonance from the central transition in the ^{7}Li NMR spectra, showing that only a single static species is present, as can be seen in Figure 4. While the chemical shift range for ^{7}Li is small, changes in the chemical shift with Li ligation environment are observed in the Li-macrocycle

(23) Johnels, D.; Andersson, A.; Boman, A.; Edlund, U. *Magn. Reson. Chem.* **1996**, *34*, 908–912.
(24) Amoureux, J. P.; Fernandez, C.; Grange, P. In *Multinuclear Magnetic Resonance in Liquids and Solids-Chemical Applications*; Granger, P., Harris, R. K., Eds.; Springer: London, 1990.

systems, as seen in the aforementioned solution state experiments. The shift from five bound nitrogen atoms (**1**) to three bound nitrogen atoms (**3**) results in an upfield shift in the isotropic chemical shift, from ~3 ppm to ~1 ppm, as shown in the figure. The presence of the additional oxygen ligand from either water or THF, compound **2**, causes a further upfield shift to ~0 ppm. These data represent the first reported solid state chemical shifts for lithium adducts of porphyrinoids. It is important to note that the chemical shift differences between the solid state and the solution phase samples are significant; this implies that the solution state structures are either different from those found in the solid state or that the samples are aggregating in solution.

The NMR spectra from quadrupole nuclei will also show an effect from the interaction of the quadrupole moment of the Li nucleus and the electric field gradient surrounding the nucleus. The magnitude of this interaction is the quadrupole coupling constant (QCC).[25] An approximate determination of the QCC values for the four compounds studied reveals that they are very similar (approximately 200 ± 50 kHz). This is expected as each lithium site has strong interactions with at least three tightly bound nitrogen atoms (Li−N bond length <2.1 Å), which will dominate the electric field gradient. The differences in the QCC across the samples then results from the remainder of the ligation environment, bonding to additional nitrogens at longer distances (hp, QCC ≈ 240 kHz), bonding to an oxygen of a solvent ligand (bzpc, QCC ≈ 150 kHz), or weak interactions with the benzene rings of the macrocycle (QCC ≈ 190 kHz). The QCC is slightly larger when water is bound to **2** than when THF is bound, indicating only a slight change in the Li environment upon substitution of the proximal ligand.

The improved solubility of the Li^+ complexes **1**−**3** over that of the unmetallated macrocycles—especially true in the case of the bzpc **2**—made possible their electrochemical characterization using cyclic voltammetry. In THF using a glassy carbon working electrode, both **1** and **3** showed completely irreversible redox processes, as shown in Figure 5. The irreversible reductions displayed by **1** at approximately −2.15 and −2.50 V (all potentials are referenced to the internal standard ferrocene and the ferrocinium/ferrocene couple) are similar to those reported by Birch and Iwamoto in their electrochemical study of the hp free base.[26]

In marked contrast to this total irreversibility is the cyclic voltammetry of **2**. As shown in Figure 6, two near-reversible one-electron waves are seen at −1.08 and −1.55 V. When recorded with instrument-determined *iR* compensation, conditions under which the internal ferrocene standard showed an anodic/cathodic peak separation of 60 mV, the peak separations for the two waves are 120 mV. Electron transfer for these two processes is thus slower than diffusion-controlled, and they do not meet the criteria for electrochemical reversibility, although the anodic and cathodic currents are equal.[27] The fact that **2** forms both a stable anion and dianion, at least on the time scale of the cyclic voltammetry experiment, is undoubtedly due to the ability of the macrocycle to delocalize charge over the three adjacent diiminoisoindoline groups, that is, the 3/4 phthalocyanine portion of the macrocycle. Of special interest are the electronic spectral changes that accompany mono- and dianion formation, a study recently undertaken in our laboratory.

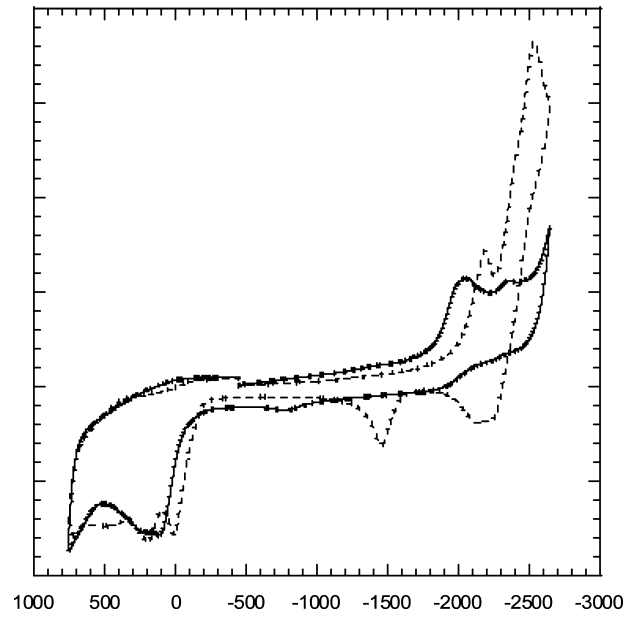

Figure 5. Cyclic voltammograms (CVs) of **3** (solid line) and **1** (dashed line) recorded in THF/0.1 M $[NBu_4][PF_6]$ using a glassy carbon working electrode. Potentials are referenced to the ferrocinium/ferrocene couple.

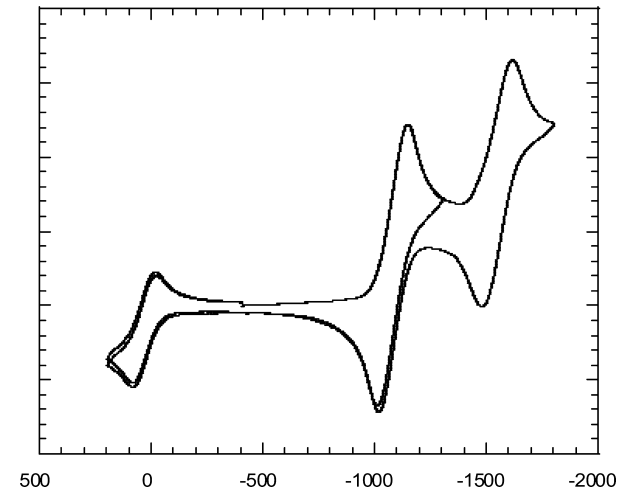

Figure 6. CV of **2** recorded in THF/0.1 M $[NBu_4][PF_6]$ using a glassy carbon working electrode. Potentials are referenced to the ferrocinium/ferrocene couple, which is shown in the CV.

In conclusion, we have successfully generated the first lithium complexes of three hp macrocycles. In all cases, a single lithium occupies the core of the ring, and charge balance is provided by protonation at external nitrogens. In the dchp and bzpc macrocycles, the internal C−H bonds are retained, affording what has been described as agostic type

(25) Duer, M. J. *Introduction to Solid-State NMR Spectroscopy*; Blackwell Publishing: Oxford, 2004.
(26) Birch, C. G.; Iwamoto, R. T. *Inorg. Chem.* **1973**, *12*, 66–73.
(27) Bard, A. J.; Faulkner, L. R. *Electrochemical Methods: Fundamentals and Applications*; John Wiley & Sons: New York, 1980, p 213.

interactions between these bonds and the lithium cations. Notably, the lithium complexes of these macrocycles have greater solubility over the free bases, which have important implications for improving the synthetic utility of reactions with hp and for improving their characterization, as shown in the electrochemistry described above. Thus, we are continuing our investigation of these lithium complexes as precursors to new metal complexes of the pyridyl and carbon substituted hp.

Experimental Section

General Methods. All reagents and solvents were purchased from Sigma, Aldrich, Acros Organics, or Strem and used without further purification. The free base hps were prepared as previously described.[14−17] Reactions and product manipulations were carried out under anaerobic conditions in a glovebox under an argon atmosphere. For the water-free reactions, anhydrous solvents were purchased from Aldrich. High resolution mass spectrometry experiments were performed at the Mass Spectrometry and Proteomics Facility of Ohio State University on a Micromass ESI-Tof II (Micromass, Wythenshawe, U.K.) mass spectrometer equipped with an orthogonal electrospray source (Z-spray) operated in positive ion mode. Sodium iodide was used for mass calibration for a calibration range of *m*/*z* 100−2000. Samples were prepared in a solution containing acidified methanol and infused into the electrospray source at a rate of 5−10 μL min^{-1}. Optimal ESI conditions were capillary voltage 3000 V, source temperature 110 °C, and cone voltage 55 V. The ESI gas was nitrogen. Data were acquired in continuum mode until acceptable averaged data was obtained. Elemental analysis was conducted at the University of Illinois, School of Chemical Sciences, Microanalysis Laboratory. All ^{1}H and ^{13}C NMR spectra were recorded on Varian VXR or GEMINI spectrometers at 300 and 75 MHz in $CDCl_3$, respectively. All solution ^{7}Li NMR data were recorded on a Varian Inova spectrometer at 116 MHz. The reference standard was LiCl in D_2O. Magic-angle spinning (MAS) ^{7}Li (155.38 MHz) solid-state NMR spectra were collected on a Varian INOVA (9.4T) spectrometer using a Varian 4 mm DR-T3 probe. One-pulse Bloch decay experiments were performed with a 6.5 μs 90° pulse width, spectral width of 0.5 MHz, and a MAS speed of 12 kHz. Samples were packed into 4 mm rotors, and the ^{7}Li chemical shifts were referenced to 1 M LiCl solution in D_2O (0 ppm). All spectra are the average of 128 scans and processed with a line broadening of 5 Hz.

Cyclic voltammetry was performed using a Bioanalytical CV-50 electrochemical analyzer and a standard three-electrode cell. THF was dried over molecular sieves and distilled from NaK alloy. A glassy carbon working electrode and a Ag/AgCl (in THF/0.1 M $[NBu_4][PF_6]$) pseudoreference electrode were used for all measurements. A scan rate of 100 mV/s was used in all experiments. Ferrocene was added to the solution at the end of each experiment, and the potentials are all referenced to the ferrocinium/ferrocene couple. Instrumentally determined *iR* compensation was used for some measurements to verify the electrochemical reversibility of ferrocene.

Single crystal X-ray diffraction data were collected at 100 K (Bruker KRYO-FLEX) on a Bruker SMART APEX CCD-based X-ray diffractometer system equipped with a Mo-target X-ray tube (λ = 0.71073 Å) operated at 2000 W power. The detector was placed at a distance of 5.009 cm from the crystal. Crystals were placed in paratone oil upon removal from the mother liquor and mounted on a plastic loop in the oil. Integration and refinement of crystal data was done using Bruker SAINT software package and Bruker SHELXTL (version 6.1) software package, respectively.[28] Absorption correction was completed by using the SADABS program. Data collection and refinement parameters for crystals of **1**−**3** are shown in Table 1.

Table 1. Crystal Data and Structure Refinement Parameters for **1**−**3**[a]

	1	**2**	**3**
formula	$C_{36}H_{25}LiN_{10}$	$C_{30}H_{20}LiN_7O$	$C_{38}H_{27}LiN_8$
formula weight	604.60	501.47	602.62
crystal syst	monoclinic	monoclinic	monoclinic
space group	$P2_1/n$	$P2_1/n$	$P2_1/n$
a, Å	14.593(3)	16.232(4)	9.459(5)
b, Å	10.444(2)	7.6569(19)	18.425(10)
c, Å	19.979(5)	18.184(4)	18.550(10)
α, deg	90	90	90
β, deg	101.078(4)	91.367(4)	102.986(10)
γ, deg	90	90	90
vol, Å^3	2988.2(12)	2259.4(10)	3150(3)
Z	4	4	4
ρ(calcd), Mg/m^3	1.344	1.474	1.271
μ, mm^{-1}	0.084	0.094	0.078
F(000)	1256	1040	1256
reflns collected	25270	16952	26174
indep. reflns	7075	4439	6862
GOF on F^2	1.035	1.048	1.004
R [$I > 2\sigma$(I)]	R1 = 0.0479, wR2 = 0.1097	R1 = 0.0551, wR2 = 0.1272	R1 = 0.0471, wR2 = 0.0995
R (all data)	R1 = 0.0720, wR2 = 0.1194	R1 = 0.0798, wR2 = 0.1363	R1 = 0.0871, wR2 = 0.1106

[a] The formula includes solvent molecules present in the asymmetric unit.

Synthesis of Lithium Hemiporphyrazine Li(Hhp)py, 1. Free base bis(pyridyl)hemiporphyrazine (H_2Hp, 0.050 g, 1.1 × 10^{-4} mol) was weighed into a flask and brought into the glovebox. This compound was mixed with a THF solution containing slightly more than 2 equiv of lithium bis(trimethylsilyl)amide (0.022 mL of a 1.0 M solution, 2.2 × 10^{-4} mol). The macrocycle dissolves upon addition of the lithium reagent. Anhydrous pyridine (20 mL) was added to this mixture, and the resultant solution was initially orange in color. After 5 h of mixing, the solution turned to a dark brown color. The reaction mixture was then filtered and reduced in volume by vacuum evaporation to 5 mL. Product was isolated by layering the solution with hexane, which produced red crystals. Yield 0.040 g (69%). High res. ESI MS (positive ion): 447.1628 M/z (M + H$^+$ − NC_5H_5, calcd 447.4076 M/z). CHN anal. Calcd for Li(Hhp)py·py ($LiC_{31}N_9H_{20}$)): C, 71.52; H, 4.17; N, 23.17. Found: C, 71.63; H, 4.09; N, 22.99. ^{7}Li NMR (Li(Hhp)py, [D_5] pyridine, δ ppm): 1.96. ^{1}H NMR ([D_6]DMSO, δ ppm): 6.52 (d, J = 7.7 Hz, 2H), 6.82 (d, J = 7.7 Hz 2H), 7.44 (m, 4H), 7.73 (m, 8H), 7.97 (m, 2H), 8.57 (m, 1H), 10.74 (s, 1H). X-ray crystallography: crystal data and structure refinement parameters are summarized in Table 1.

Synthesis of Lithium Benziphthalocyanine Li(H_2bzpc)H_2O, 2. Free base benziphthalocyanine (H_3bzpc, 0.050 mg, 1.05 × 10^{-4} mol) was weighed into a flask and brought into the glovebox. This compound was mixed with a THF solution containing slightly more than 2 equiv of lithium bis(trimethylsilyl)amide (0.027 mL of a 1.0 M solution, 2.7 × 10^4 mol). This resultant mixture was then diluted with an additional 20 mL of THF. The insoluble free base dissolved as the reaction proceeded, and the resultant solution was red in color. The reaction proceeded over 5 h, and the solution became a darker red color. The resultant solution was then filtered and reduced in volume by vacuum evaporation to 5 mL. Product was isolated by recrystallization from nonanhydrous THF by layering the solution with heptane, which produced X-ray quality red plates. Yield 0.042 g (76%). ESI MS (positive ion): 508.1 M/z

(28) Sheldrick, G. M. *SHELXTL, Crystallographic Software Package*, Version 6.10; Bruker-AXS: Madison, WI, 2000.

(M − Li + CH_3OH, calcd 508.1 M/z). CHN anal. Calcd for Li(H_2bzpc)H_2O ($LiC_{30}N_7H_{20}O$): C, 71.85; H, 4.02; N, 19.55. Found: C, 72.85; H, 4.02; N, 17.86. ^{7}Li NMR (Li(H_2bzpc)THF, [D_8]THF, δ ppm): 3.11. ^{1}H NMR ([D_6]DMSO, δ): 1.73 (p, THF), 1.67 (s, H_2O), 3.60 (t, THF), 6.97 (q, J = 7.9, 13.7 Hz, 2H), 7.20 (t, J = 7.8 Hz, 1H), 7.42 (m, 8H), 7.55 (m, 1H), 7.82 (m, 4H), 8.39 (s, 1H), 8.68 (s, 1H). X-ray crystallography: crystal data and structure refinement parameters are summarized in Table 1.

Synthesis of Lithium Dicarbahemiporphyrazine Li(dchp)L, (L = py, THF) 3. The same procedure was used as for **1** but with the dicarbahemiporphyrazine free base (H_2dchp, 0.050 mg, 1.1 × 10^{-4} mol). The H_2dchp ligand is not as soluble as the previous two macrocycles, so the temperature of the solution was increased to 50 °C and the mixture stirred for 5 h to drive the reaction. The resultant solution was yellow in color. The resultant solution was then filtered and stripped of solvent by vacuum evaporation. Crystals of the product were grown from nonanhydrous THF/hexanes to afford the THF-coordinated product, which was used for elemental analysis and mass spectrometry; anhydrous THF was used for the NMR analysis. X-ray quality crystals were grown from anhydrous pyridine/hexanes. Yield 0.035 g (60%). High res. ESI MS (positive ion): 445.1756 M/z (M + H, calcd 445.4321). CHN anal. Calcd for Li(dchp)THF·H_2O ($LiC_{32}N_6H_{27}O_2$): C, 71.90; H, 5.09; N, 15.72. Found: C, 71.95; H, 5.35; N, 14.15. ^{7}Li NMR (Li(Hdchp)THF, [D_8]THF, δ ppm): 2.75, (Li(Hdchp)py, [D_5] pyridine, δ ppm): 1.54. ^{1}H NMR ([D_8]THF, δ): 6.85 (d, J = 7.4 Hz, 4H), 7.22 (t, J = 7.9 Hz, 2H), 7.32 (t, J = 7.9 Hz, 2H), 7.67 (m, 4H), 7.98 (m, 4H), 9.14 (s, 1H).

Acknowledgment. This work was supported by the NSF (CHE-0616416). We wish to also acknowledge NSF Grant CHE-0116041 used to purchase the Bruker-Nonius diffractometer.

Supporting Information Available: Crystallographic data for complexes **1**−**3** (CIF). This material is available free of charge via the Internet at http://pubs.acs.org.

IC800817X